Amount of Free Carbon at End of Solidification in Spheroidal Graphite Iron Castings

Tomokatsu Kotani [1*], Kazuya Edane [2], Keita Iwakado [3], Haruki Itofuji [4]

[1*] Yanmar Casting Technology Co., Ltd., Matsue City, Japan
[2] Tsuchiyoshi Industry Co., Ltd., Ochi County, Japan
[3] Ota Chuzosho Co., Ltd., Yamagata County, Japan
[4] Adstefan Casting Solution Center, Tohoku University, Sendai City, Japan

ABSTRACT

To clarify why shrinkage-free, spheroidal graphite iron castings can be obtained without risers only for casting modulus (*M*) greater than 3.0 cm, free carbon as graphite precipitated up to the end of solidification was analyzed for test castings with *M* = 0.5–5.0 cm. Each casting was quenched in water just after solidification. Samples were taken from the castings and their free-carbon content was analyzed according to JIS G 1211-5 (ISO/TR 10719). The amount of free carbon was similar for all castings. This finding is in contrast with that of a previous study, in which the free-carbon value in castings with *M* < 3.0 cm was less than that in castings with *M* > 3.0 cm. The influence of inoculant fading time on graphite precipitation was also investigated.

Keywords: free carbon, riser design, spheroidal graphite iron, shrinkage, inoculation

INTRODUCTION

Graphite precipitation during solidification has a strong influence on shrinkage in graphite iron castings[1]. If expansion is effectively used, it is possible to use a riser-less design[2-7]. However, it is generally believed that riser-less designs are not feasible for castings with casting modulus (*M* = *V*/*S*, where *V* is the volume and *S* is the surface area) less than 2.5 cm. According to Goto *et al*.[7] and Chang[6], this is because the amount of graphite precipitation as free carbon is insufficient as a shrinkage countermeasure for *M* < 2.5 cm, whereas above for *M* > 2.5 cm, carbon is saturated in the austenite and there is a high degree of graphite precipitation. In their studies, free carbon just after solidification was analyzed by converting 2D morphological images to 3D volumes, and then converting the volume to a mass fraction. In this study, free carbon as graphite was extracted from samples that were quenched just after solidification and analyzed using the infrared absorption method.

EXPERIMENTAL PROCEDURE

1. INFLUENCE OF IMMEDIATELY AFTER MG-TREATED IRON

1.1 FOUNDRY EXPERIMENTS

Solidification curves for sample castings with *M* = 0.5–5.0 cm were first determined. The modulus and dimensions of the sample castings are shown in Table 1 and the cast design is shown in Fig. 1.

Table 1 Sizes of sample castings with different modulus

M (cm)	Diameter × height (mm)
0.5	30 × 30
1.0	60 × 60
2.0	120 × 120
3.0	180 × 180
4.0	240 × 240
5.0	300 × 300

Molten iron was prepared using a 5-ton high-frequency induction furnace and was treated with 1.25 wt.% Fe-Si-6.1mass%Mg and 0.4 wt.% Fe-47mass%Si using the sandwich method during tapping. Steel-scrap chips of 1.0 wt. % were covered on the alloys. Mg-treated molten iron was poured into a furan–silica sand

mold at a temperature of about 1380 °C (1653 K). A solidification curve of each sample casting was measured at the center of the sample to use as master curves for the subsequent quenching experiments.

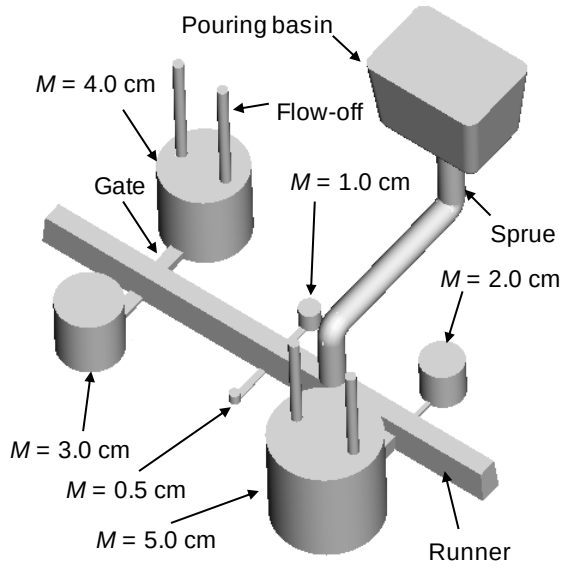

Fig. 1 Design for sample castings in a furan–silica mold.

1.2 LABORATORY EXPERIMENTS

The sample castings were quenched after solidification and the amount of free carbon was determined. Molten iron was prepared using a 30-kg high-frequency induction furnace. The chemical composition was the same as that used in the first melting in the foundry, with the same raw materials and treatment with the same alloys. The samples that were analyzed for free carbon were quenched to maintain the conditions at the end of solidification. Therefore, these samples were small enough to quench. The samples were divided into two groups. Samples in the first group had M = 0.5–2.0 cm. These samples were molded with furan silica sand and Mg-treated molten iron. Their solidification behavior was monitored with K-type thermocouples at the center of the samples. They were quenched in water at about 1100 °C (1373 K). Samples in the other group had M = 3.0–5.0 cm.

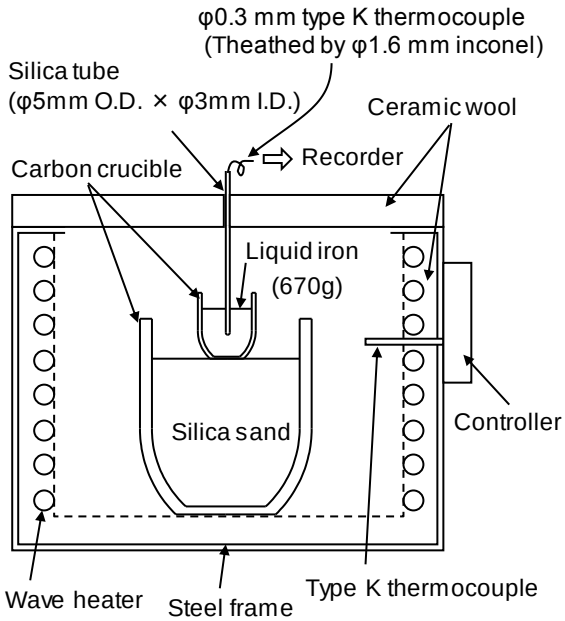

Fig. 2 Experimental apparatus for the laboratory experiments.

As shown in Fig. 2, Mg-treated iron was poured into graphite crucibles and cooled in the control furnace, reproducing the solidification curves measured in the foundry. Monitoring and quenching were conducted using the same procedure as described above. Sections of 10 × 10 × 1 mm^3 were taken from the samples near the thermocouple using a micro-cutter and the free carbon (*i.e.*, graphite) was analyzed according to JIS G1211-5 (ISO/TR 10719). The free carbon was filtered out from the acid resolution liquid using a 0.3-μm glass-fiber filter. The total carbon was analyzed using the infrared absorption method (CS-LS600, Leco Corp.).

2. INFLUENCE OF POST-INOCULATION

The influence of post-inoculation on graphite precipitation was evaluated for a constant modulus. The size of the sample castings is shown in Fig. 3. Base iron was prepared using a 3-ton high-frequency induction furnace. The chemical composition was set to be similar to that use in the foundry. Molten iron (900 kg) was treated with the same alloys as in the laboratory experiments using the sandwich method with a 1-ton ladle. Mg-treated molten iron was held for approximately 30 minutes at a temperature of 1420 °C (1693 K) and was poured into the cup shown in Fig. 3 in six 6-minute steps. The samples were quenched in water at about 1000 °C (1273 K) to avoid precipitation of ledeburite, which causes undercooling and a dependence on inoculant fading time[7,8]. The free carbon was analyzed using the same method as in the laboratory experiments.

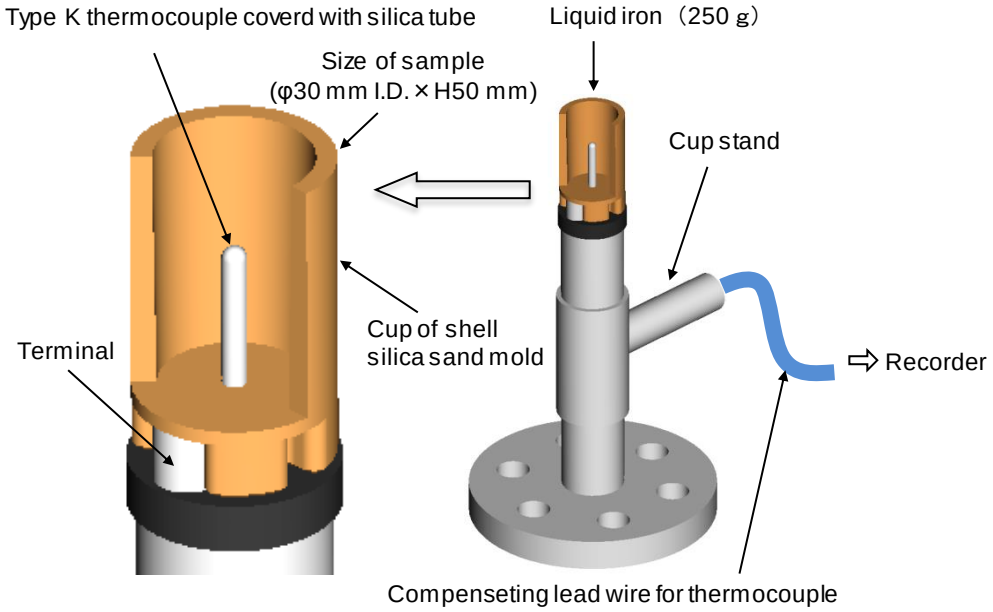

Fig. 3 Experimental apparatus used for thermal analysis.

RESULTS AND DISCUSSION

The chemical composition of Mg-treated molten iron in the foundry is given in Table 2 and the corresponding solidification curves are shown in Fig. 4. Undercooling of the eutectic temperature was observed for sample castings with $M < 3.0$ cm. The eutectic temperatures of the samples with $M = 3.0$–5.0 cm were almost constant.

Table 2 Chemical composition of the sample used in the foundry experiments (mass%)

C	Si	Mn	P	S	Mg
3.33	2.41	0.32	0.025	0.010	0.047

The chemical composition of the Mg-treated molten iron used in the laboratory experiment is shown in Table 3. The solidification curves of the sample castings measured in the laboratory are shown in Fig. 5. Fig. 5 indicates that the solidification behavior shown in Fig. 4 is reproduced well, except at the early stage of the

solidification curve. This is because the sampling temperature in the laboratory was higher than that in the foundry.

The microstructures of the sample castings quenched in water after solidification are shown in Fig. 6. The microstructures were observed at a position near the thermocouple. Well-formed spheroidal graphite was obtained, as shown in Fig. 6. There was a small amount of the ledeburite structure in the sample castings with M = 3.0–5.0 cm but not in the samples with M = 0.5–2.0 cm. The existence of the ledeburite structure means that solidification was not complete when the sample castings were quenched. However, it is considered that the amount of ledeburite has almost no influence on the results of this study.

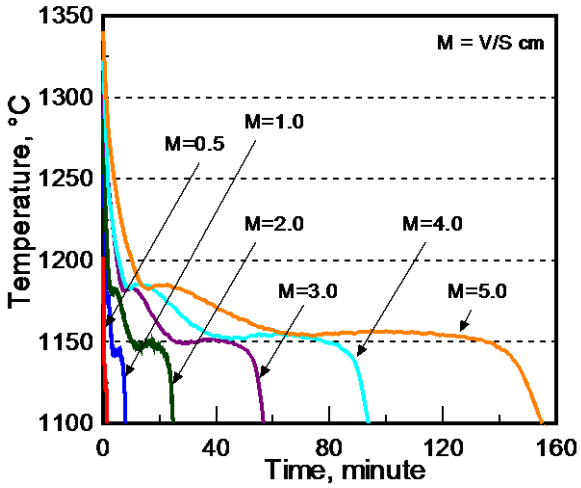

Fig. 4 Solidification curves for sample castings with M = 0.5–5.0 cm used in the foundry experiments.

Table 3 Chemical composition of samples used in the laboratory experiments (mass%)

Sample casting M (cm)	C	Si	Mn	P	S	Mg
0.5	3.46	2.38	0.29	0.022	0.015	0.046
1.0 2.0 4.0	3.42	2.45	0.30	0.024	0.010	0.047
3.0	3.39	2.41	0.32	0.029	0.015	0.041
5.0	3.46	2.36	0.27	0.029	0.015	0.050

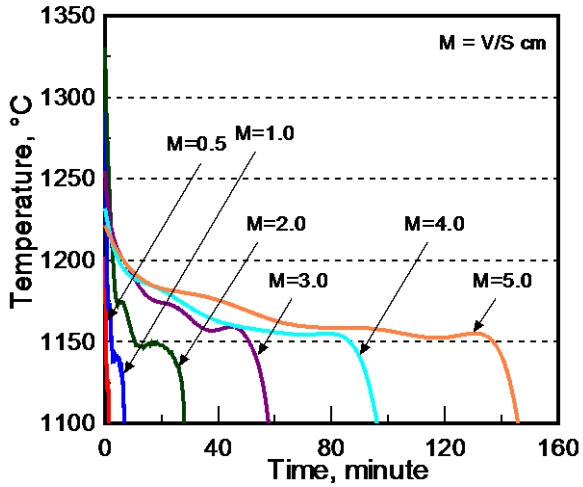

Fig. 5 Solidification curves for samples used in the laboratory experiments.

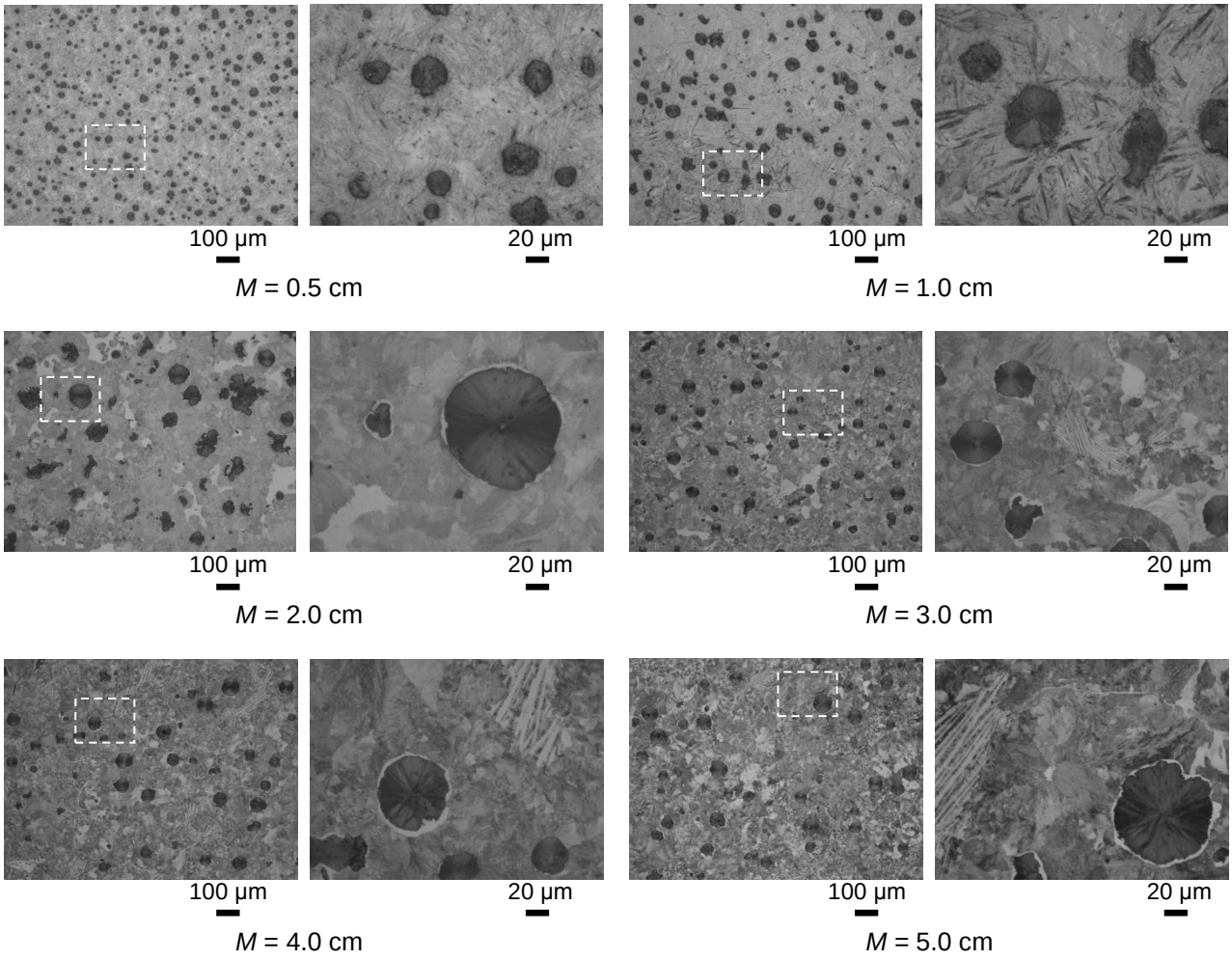

Fig. 6 Microstructures of each sample casting that were quenched in water at 1100 °C (etched with 5 vol.% nital).

Because of the variation in the chemical compositions among the sample castings used in the laboratory experiments, the results are given as a ratio of the free carbon to the total carbon (referred to as the free/total carbon ratio). The modulus was converted to a solidification time according to the results of the thermal analysis. The relationship between the ratio of free to total carbon and the solidification time is shown in Fig. 7.

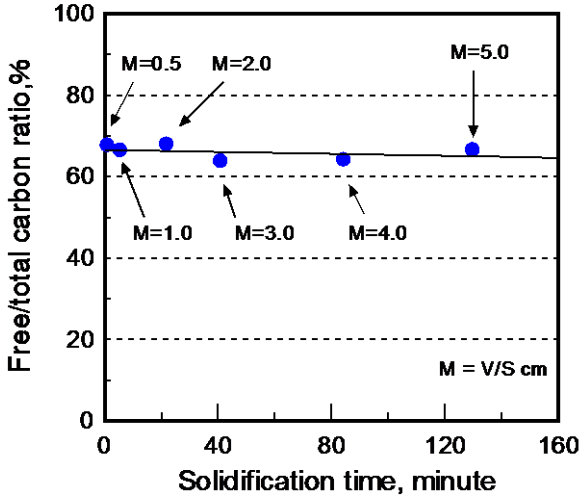

Fig. 7 Relationship between solidification time and free/total carbon ratio.

The ratio of the free to total carbon is almost the same for all sample castings. This is in contrast to previously reported results, where the amount of graphite decreased because of hyper-saturation of carbon in austenite when the solidification time was less than 20 minutes[6,7]. However, in these studies, the graphite ratio was obtained by 2D morphological image analysis, which is less accurate because the results depend on the polished condition of the samples. The chemical composition of Mg-treated molten iron after different inoculant fading times is shown in Table 4. There was almost no decrease in the Mg content of the samples, even after 30 minutes. The cooling curves are shown in Fig. 8.

Table 4 Chemical composition for different inoculant fading times of Mg-treated molten iron (mass%)

Inoculant fading time (minute)	C	Si	Mn	P	S	Mg
0.5	3.49	2.49	0.32	0.018	0.013	0.056
6.0	3.49	2.50	0.32	0.018	0.013	0.055
12.0	3.50	2.50	0.32	0.018	0.013	0.053
18.0	3.49	2.51	0.33	0.019	0.013	0.051
24.0	3.51	2.48	0.32	0.018	0.013	0.049
30.0	3.51	2.47	0.32	0.018	0.014	0.050

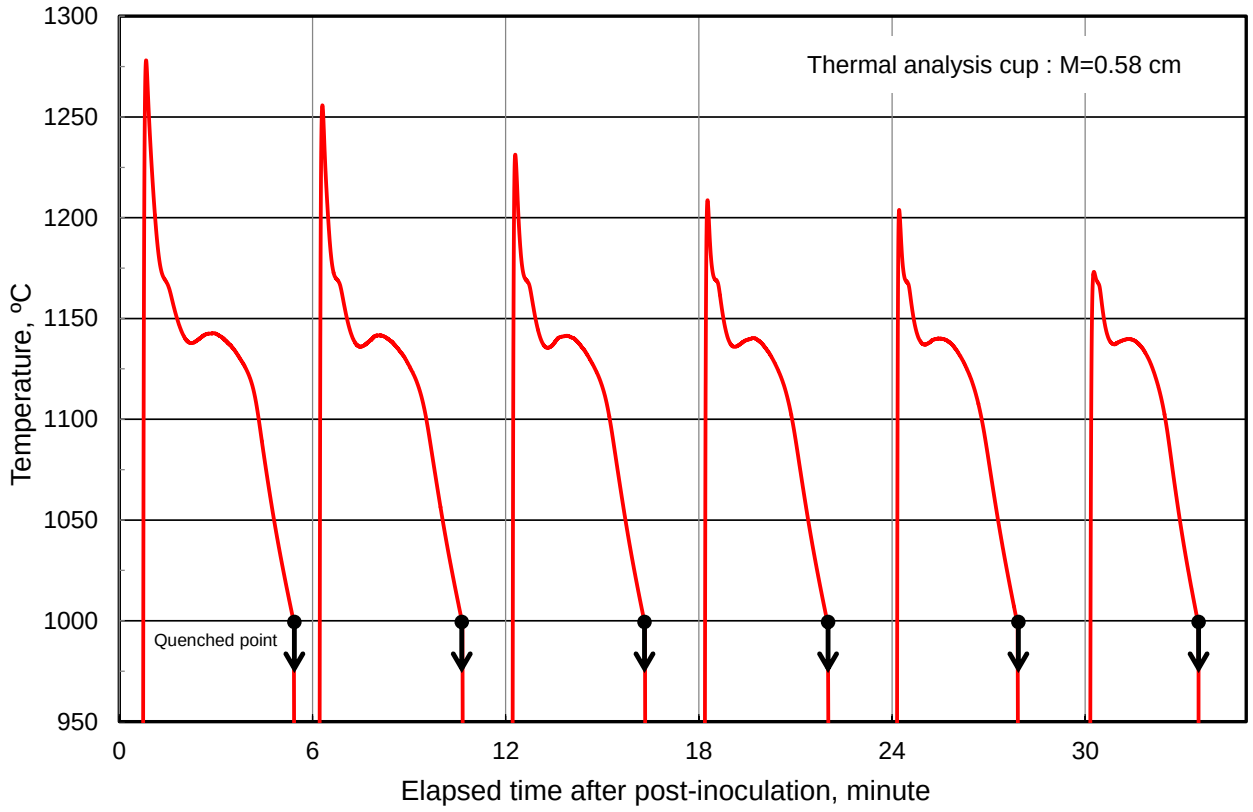

Fig. 8 Solidification curves for different inoculant fading times.

As shown in Fig. 8, there was almost no change in the solidification curves for the different inoculant fading times. Using the same procedure as described above, the microstructures were observed of all samples and their free carbon content was analyzed. Typical microstructures of castings quenched in water after solidification are shown in Fig. 9. All samples displayed fully formed spheroidal graphite structures without the precipitation of ledeburite. The relationship between the ratio of free to total carbon and the elapsed time post-inoculation is shown in Fig. 10. These results again demonstrate that there was almost no variation among the samples.

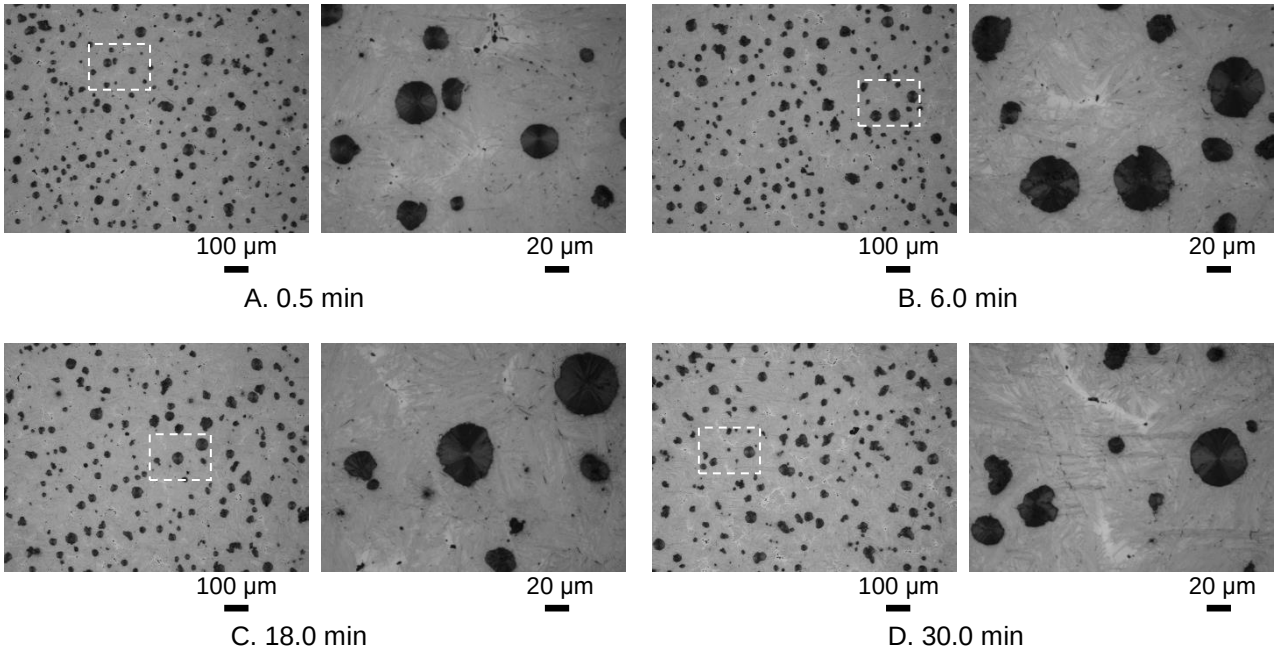

Fig. 9 Microstructures of sample castings that were quenched in water at 1000 °C (etched with 5 vol.% nital).

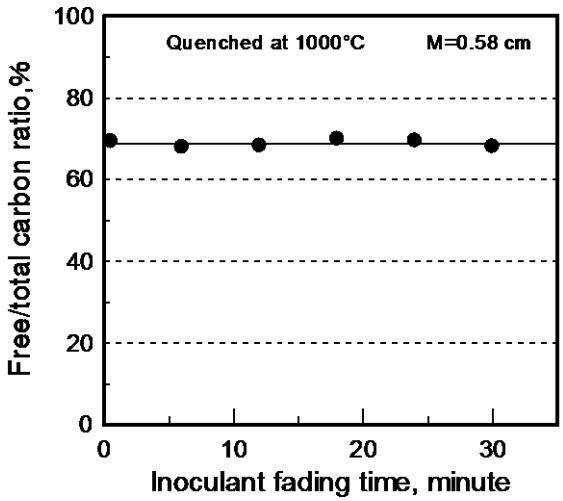

Fig. 10 Relationship between the inoculant fading time and free/total carbon ratio.

The validity of the test results was considered. According to Heine[9], and Hocheid and Poupeau[10], the carbon solubility in austenite in laboratory experiments can be defined using Eqns 1 and 2. The carbon solubility in austenite calculated from Eqns 1 and 2 is shown in Table 5. The values obtained in this study are also provided. Assuming that these equations are reasonable, the results of this study indicate that carbon is not saturated in the austenite.

$$C\gamma \text{ mass } \% = 2.1 - 0.217Si \qquad \text{Eqn. 1}$$

$$C\gamma \text{ mass } \% = 2.045 - 0.178Si \qquad \text{Eqn. 2}$$

The Fe–C phase diagram for 2.5 mass% Si is shown in Fig. 11[11]. When the results of this study are plotted on this phase diagram, they all appear in the austenite region.

Table 5 Calculated carbon solubility in austenite for different silicon contents (mass%)

Silicon content		2.45	2.41	2.36	2.38
Carbon solubility in austenite	Eqn. 1 [9]	1.57	1.58	1.59	1.58
	Eqn. 2 [10]	1.61	1.62	1.62	1.62
	This study (mean;*n* = 2)	1.16	1.23	1.16	1.12

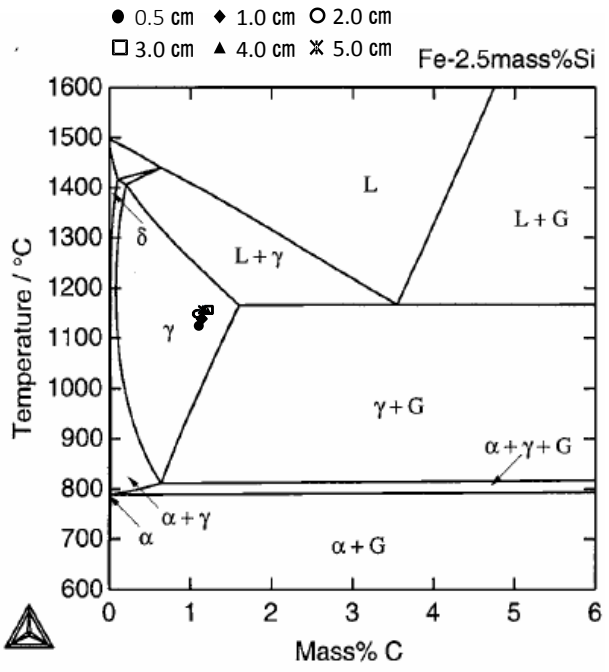

Fig. 11 Relationship between carbon solubility and the eutectic temperature in the Fe–C–2.5mass%Si phase diagram[11].

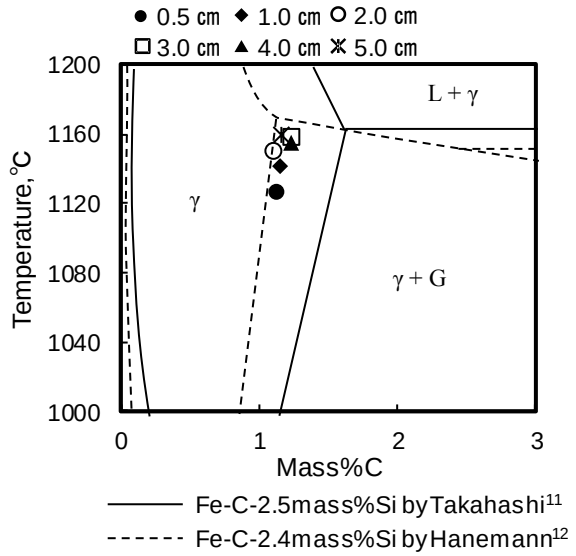

Fig. 12 Fe–C–Si phase diagram at carbon saturation in austenite.

When plotted on the Fe–C–2.4mass%Si phase diagram proposed by Hanemann and Jass[12], the results from this study lie slightly above the carbon saturation line in austenite, as shown in Fig. 12. The enlargement of the carbon saturation area in austenite of the Fe–C–2.5mass%Si phase diagram is also shown in Fig. 12.

As mentioned above, it is clear that the amount of free carbon as graphite, which is related to shrinkage, is almost the same among the different castings, even though their modulus differs greatly. Hyper-saturation of carbon in austenite did not occur. However, when the modulus of the spheroidal graphite iron casting is less than 3.0 cm, there is a high probability of the occurrence of shrinkage defects. It is considered here that free carbon is necessary, but alone it is not sufficient as a shrinkage countermeasure in castings. The timing of precipitation and the amount of free carbon during the solidification progress may be related to shrinkage defects.

The amount of free carbon as graphite may increase in terms of nodule count when chillers are used and post-inoculation is effectively conducted. However, it was found that even if molten iron is held for 30 minutes after inoculation, the amount of free carbon remained almost unchanged. For castings with modulus less than 3.0 cm, undercooling of the eutectic temperatures occurred. By contrast, this did not occur in castings with modulus greater than 3.0 cm. This might suggest that the shrinking behavior differs between samples in these two modulus regimes. If graphite nucleates and grows on the walls of Mg gas bubbles, smaller modulus castings may exhibit less volumetric expansion than castings with larger modulus[13]. This is because of the large amount of precipitated graphite in the Mg gas bubbles and the fact that graphite will not grow much larger than the bubbles.

CONCLUSIONS

Direct quantitative analysis was conducted on samples taken just after the completion of solidification in spheroidal graphite iron castings. The following conclusions are drawn:

1. The amount of free carbon was almost equal among all castings, even though their modulus differed greatly;
2. The eutectic temperature was almost constant in castings with modulus greater than 3.0 cm;
3. The eutectic temperature decreased when the casting modulus was less than 3.0 cm;
4. The amount of free carbon at the end of solidification did not directly relate to shrinkage;
5. The inoculant fading time had no effect on the amount of free carbon but did influence the solidification behavior.

REFERENCES

1. M.J. Gough, J. Morgan, “Feeding Ductile Iron Castings-Some Recent Experiments,” *American Foundry Society Transactions,* vol. 84 (1976), pp. 351–384.
2. S.I. Karsay, “Ductile Iron I-Production,” *Quebec Iron and Titanium* (1976).
3. S.I. Karsay, “Ductile Iron III-Design of Gating System and Riser,” *Quebec Iron and Titanium* (1981).
4. M. Taffazzoli, V. Kondic, “Making Sound Ductile Iron Castings without Risers,” *Foundry Management and Technology*, vol. 104, 12 (1976), pp. 86ff.
5. M. Taffazzoli, V. Kondic, “Volume Contraction and Shrinkage Cavities Behavior in Ductile Iron Castings,” *AFS International Cast Metals Journal*, vol. 2, 12 (1977), pp. 41–47.
6. B. Chang, “The Riserless Design of Ductile Cast Iron,” *Imono*, vol. 55, 2 (1983), pp. 113–120.
7. A. Goto, T. Aizawa, S. Okada, “On the Amount of Graphite Formed during Freezing and Cooling in Spheroidal Graphite Cast Iron,” *Imono*, vol. 50, 6 (1978), pp. 345–349.
8. T. Owadano, K. Torigoe, I. Kanzaki, “The Interrelationship of Solidification time, Undercooling and the Number of Graphite Nodules in Spheroidal Graphite Cast Iron,” *Imono*, vol. 48, 9 (1976), pp. 563–567.
9. R.W. Heine, “The Carbon Equivalent Fe-C-Si Diagram and its Application to Cast Irons,” *AFS Cast Metals Research Journal*, vol. 7 (1971), pp. 49–54.
10. B. Hocheid, P. Poupeau, “Diagrammes d’équilibre: Alliages ternaires,” (1978).
11. T. Takahashi, K. Oikawa, “The Fe-C-Si System Ternary Calculation Phase Diagram,” *Tohoku Industrial Technology Laboratory T/R*, vol. 23 (1999), pp. 192−197.

12. H. Hanemann, H. Jass, “Ueber das System Eisen-Eisensilizid FeSi-Graphit,” *Giesserei*, vol. 25 (1938), pp. 293–299.
13. H. Itofuji, “Study on Graphite Spheriodization in Cast Irons,” Doctoral Thesis, Kyoto University (1993).

ACKNOWLEDGEMENTS

The authors appreciate the help given by S. Moritake and Y. Miyamoto of UBE Steel Co., Ltd., in analyzing the large number of samples and materials tested. We also thank the members of Tsuchiyoshi Industry Co., Ltd., for technical assistance with the experiments. Finally, the first author gratefully acknowledges the work of past and present members of the Quality Engineering Group (T. Ogino, Y. Mimura, K. Ishikawa, and R. Sato).